

Stabilization of Carbanions. 1. Origin of the Increased Acidity of Dimethyl Sulfide As Compared to Dimethyl Ether

Kenneth B. Wiberg* and Henry Castejon

Contribution from the Department of Chemistry, Yale University, New Haven, Connecticut 06520

Received June 6, 1994[®]

Abstract: The origin of the increased acidity of dimethyl sulfide as compared to dimethyl ether was studied via ab initio geometry optimizations at the MP2/6-31+G* level followed by MP2/6-311++G** energy calculations. The further increases in acidity on going from dimethyl sulfide to dimethyl sulfoxide and dimethyl sulfone also were examined. With dimethyl ether, loss of a proton giving the carbanion leads to an increase in the O–CH₂[–] bond length and places the lone pair syn to the methyl group. On the other hand, the conversion of dimethyl sulfide to the anion leads to a decrease in the S–CH₂[–] bond length and gives a small preference for the lone pair to be anti to the methyl group. With the ether, the C–O bond order is not significantly affected by formation of the anion, but with the sulfide, there is a considerable increase in bond order. With CH₃SCH₂[–], a large rotational barrier was found, and during rotation there were large changes in the S–CH₂[–] bond length and in the pyramidalization at the anionic carbon. These data indicate that negative hyperconjugation is important in stabilizing CH₃SCH₂[–] but not CH₃OCH₂[–]. The role of d and diffuse functions in stabilizing the neutral molecules and their anions was studied via charge density difference plots. The d functions served mainly to transfer charge from lone pairs to bonding regions and had little effect on the relative energies. The stabilization of the carbanion by sulfur is lost when the charge is localized by a nearby lithium cation, but only part of the energy change appears to be due to the greater chelation effect of oxygen vs sulfur. The acidity of 1,3-dioxane and of 1,3-dithiane also was studied.

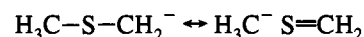
1. Introduction

Dimethyl ether (**1**) is considerably less acidic than dimethyl sulfide (**2**). The heats of ionization (ΔH_{acid}) have been measured in the gas phase and are 407 ± 2 and 393 ± 3 kcal/mol, respectively.¹ This increased acidity of a carbon adjacent to a sulfur has received considerable use in synthetic applications.² However, it appears unusual in view of the relatively large electronegativity difference between carbon and oxygen, and the negligible difference between carbon and sulfur.³ The high electronegativity of oxygen would be expected to deplete the charge density at the methylene carbon, thus stabilizing the carbanion formed by proton loss. The effect is seen in comparing dimethyl ether with propane, where the heat of ionization of a methyl CH of propane is 420 ± 3 kcal/mol. This type of stabilization cannot be provided by sulfur.

Further increases in acidity are found with the oxidized forms of dimethyl sulfide, the sulfoxide **3**, and the sulfone **4**. The corresponding anions have heats of ionization of 374 ± 3 and 366 ± 3 kcal/mol, respectively.

In order to gain more information concerning the difference in acidity between **1** and **2**, we have carried out a set of ab initio calculations. The origin of the difference has previously been studied by several investigators, and three different mechanisms have been proposed: polarization,^{4–8} d orbital

participation,⁹ and negative hyperconjugation.^{7,9,10} The polarization mechanism depends on the larger size and higher polarizability of sulfur as compared to oxygen, and might allow the charge distribution about sulfur to shift so as to stabilize the adjacent carbanion. This mechanism has been used to explain the higher gas-phase acidity of *tert*-butyl alcohol as compared with methyl alcohol.¹¹ The d orbital participation model is suggested by the observation that the geometry of S–CH₂[–] bonds is strongly affected by the inclusion of d polarization functions in the basis set.⁹ The hyperconjugation mechanism involves double bond–no bond resonance structures such as



or the equivalent MO model of electrons from the carbanion center being donated into the adjacent C–S σ^* antibonding orbital. Although the polarization model is the most generally accepted, it appeared important to gain further information on the origin of the effect, and therefore, we have investigated the problem using both a higher theoretical level and a different method of analysis. It might be noted that many of the previous studies used HSCH₂[–] as a model,^{3–5,9} and it is possible that the interactions will be different than those in CH₃SCH₂[–].

[®] Abstract published in *Advance ACS Abstracts*, October 1, 1994.

(1) Lias, S. G.; Bartmess, J. E.; Liebman, J. F.; Holmes, J. L.; Levin, R. D.; Mallard, W. G. *Gas Phase Ion and Neutral Thermochemistry*. *J. Phys. Chem. Ref. Data* **1988**, *17*, Suppl. 1. A decrease in proton affinity indicates an increase in acidity. Although the differences may appear to be small differences in large numbers, it should be remembered that much of the energy is associated with the high electrostatic energy of a proton in the gas phase. Thus, the differences in energy are quite significant.

(2) Corey, E. J.; Seebach, D. *Angew. Chem., Int. Ed. Engl.* **1965**, *4*, 1075, 1077. Corey, E. J.; Erickson, B. W. *J. Org. Chem.* **1971**, *36*, 3553.

(3) Allred, A. L.; Rochow, E. G. *J. Inorg. Nucl. Chem.* **1958**, *5*, 264.

(4) Streitwieser, A.; Williams, J. E., Jr. *J. Am. Chem. Soc.* **1975**, *97*, 191.

(5) Lehn, J.-M.; Wipff, G. *J. Am. Chem. Soc.* **1976**, *98*, 7498.

(6) Bernardi, F.; Csizmadia, I. G.; Mangini, A.; Schlegel, H. B.; Whangbo, M.-H.; Wolfe, S. *J. Am. Chem. Soc.* **1975**, *97*, 2209.

(7) Schleyer, P. v. R.; Clark, T.; Kos, A. J.; Spitznagel, G. W.; Rohde, C.; Arad, D.; Houk, K. N.; Rondan, N. G. *J. Am. Chem. Soc.* **1984**, *106*, 6467.

(8) Hopkinson, A. C.; Lien, M. H. *J. Org. Chem.* **1981**, *46*, 998. Larson, J. R.; Epiotis, N. D. *J. Am. Chem. Soc.* **1981**, *103*, 410. Durmaz, S. *J. Organomet. Chem.* **1975**, *96*, 331.

(9) Wolfe, S.; LaJohn, L. A.; Bernardi, F.; Mangani, A.; Tonachini, *Tetrahedron Lett.* **1983**, *24*, 3789. Wolfe, S.; Stolow, A.; LaJohn, L. A. *Tetrahedron Lett.* **1983**, *24*, 4071. They report geometry optimizations for dimethyl sulfide and its anion at the HF/3–21G* level.

(10) Schleyer, P. v. R.; Kos, A. J. *Tetrahedron* **1983**, *39*, 1141.

(11) Brauman, J. I.; Riveros, J. M.; Blair, L. K. *J. Am. Chem. Soc.* **1971**, *93*, 3914.

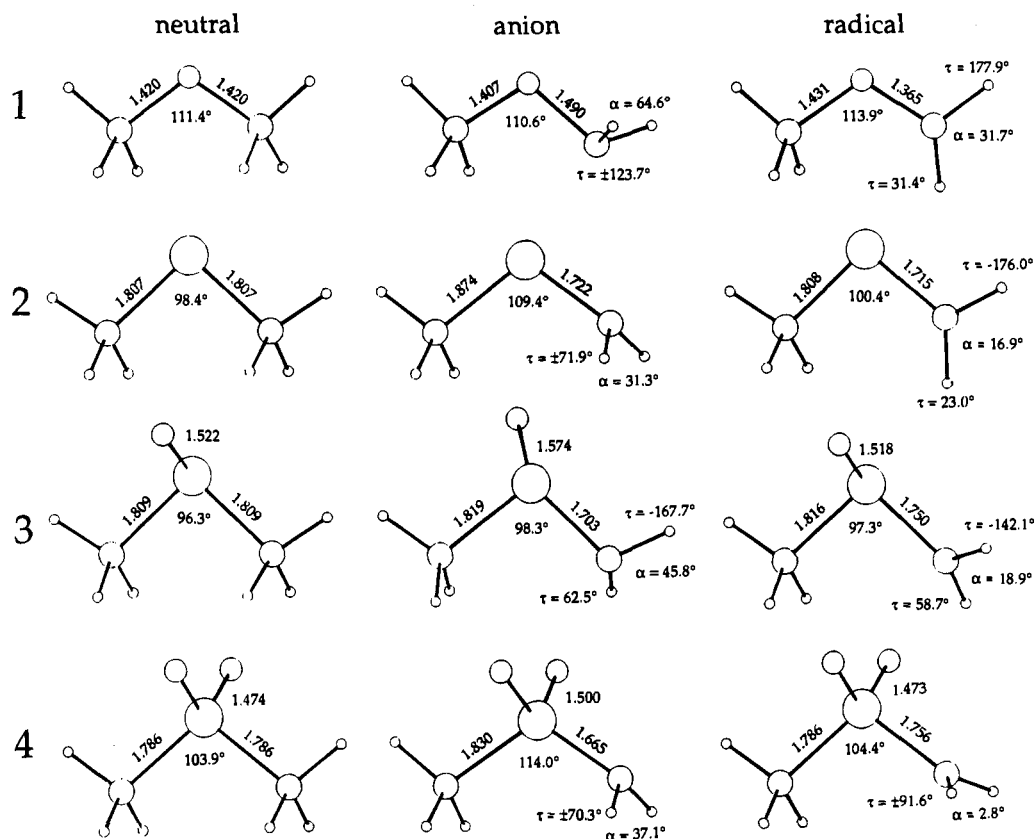


Figure 1. MP2/6-31+G* calculated structures of dimethyl ether (1), dimethyl sulfide (2), dimethyl sulfoxide (3), dimethyl sulfone (4), and their radicals and anions.

Table 1. Calculated Energies^a

compd	ZPE ^c	MP2/6-31+G*	MP2/6-311++G**	MP3/6-311++G**	ΔH_{acid}^d	
					calc	obs
dimethyl ether (1)	48.2	-154.514 63	-154.623 68	-154.650 07	412	407 ± 2
anion (1a)	38.0	-153.844 09	-153.951 16	-153.971 61		
radical (1r)	39.7	-153.864 30	-153.965 02	-153.989 49		
radical ^b		-153.835 22				
dimethyl sulfide (2)	45.6	-477.125 89	-477.231 05	-477.270 29	396	393 ± 3
anion (2a)	36.3	-476.483 16	-476.585 96	-476.616 85		
radical (2r)	37.0	-476.477 35	-476.573 47	-476.611 27		
radical ^b		-476.458 90				
dimethyl sulfoxide (3)	48.0	-552.130 05	-552.262 91	-552.289 23	376	374 ± 3
anion (3a)	39.4	-551.521 19	-552.650 65	-551.668 77		
radical (3b)	39.2	-551.469 73	-551.593 22	-551.619 22		
radical ^b		-551.450 74				
dimethyl sulfone (4)	51.6	-627.174 44	-627.337 33	-627.349 12	367	366 ± 3
anion (4a)	42.7	-626.577 59	-626.737 65	-626.744 56		
radical (4b)	42.7	-626.509 63	-626.663 61	-626.675 24		
radical ^b		-626.489 08				
propane	62.0	-118.664 88	-118.767 43		414	420 ± 3
1-anion	51.7	-117.987 85	-118.090 87			

^a The total energies are given in hartrees, and the zero-point energies and gas-phase acidities are given in kcal/mol. The larger basis set MP calculations were carried out using the MP2/6-31+G* geometries. ^b Calculated at the anion geometry. ^c From HF/6-31+G* calculations scaled by 0.893. ^d Based on the MP2/6-311++G** energies: see text. The observed values were taken from ref 1.

2. Structural Changes

The structures and energies of the parent compounds and their corresponding free radicals and anions were obtained at the MP2/6-31+G* level which is known to reproduce experimental data satisfactorily for carbanions.¹² The MP2 optimized structures are significantly different than those obtained at the RHF theoretical level. Single-point MP2 and MP3 calculations were carried out with the 6-311++G** basis set using the MP2/6-31+G* geometries. The frozen core option was used for all of the MP calculations. Zero-point energies were estimated from HF/6-31+G* calculations, scaling the frequencies by 0.893. The

structures are shown in Figure 1 and the energies are given in Table 1. The proton affinities were calculated from the energies, and the MP2/6-311++G** ΔH_{acid} values are in good agreement with the experimental values (Table 1). The MP3 energies give ΔH_{acid} that are 3–5 kcal/mol larger, and are less satisfactory. Pople et al. have found that MP2 relative energies are often more satisfactory than MP3.¹³

It is frequently possible to obtain useful information on intramolecular interactions by examining changes in structural

(12) Hehre, W. J.; Radom, L.; Schleyer, P. v. R.; Pople, J. A. *Ab Initio Molecular Orbital Theory*; Wiley: New York, 1986.

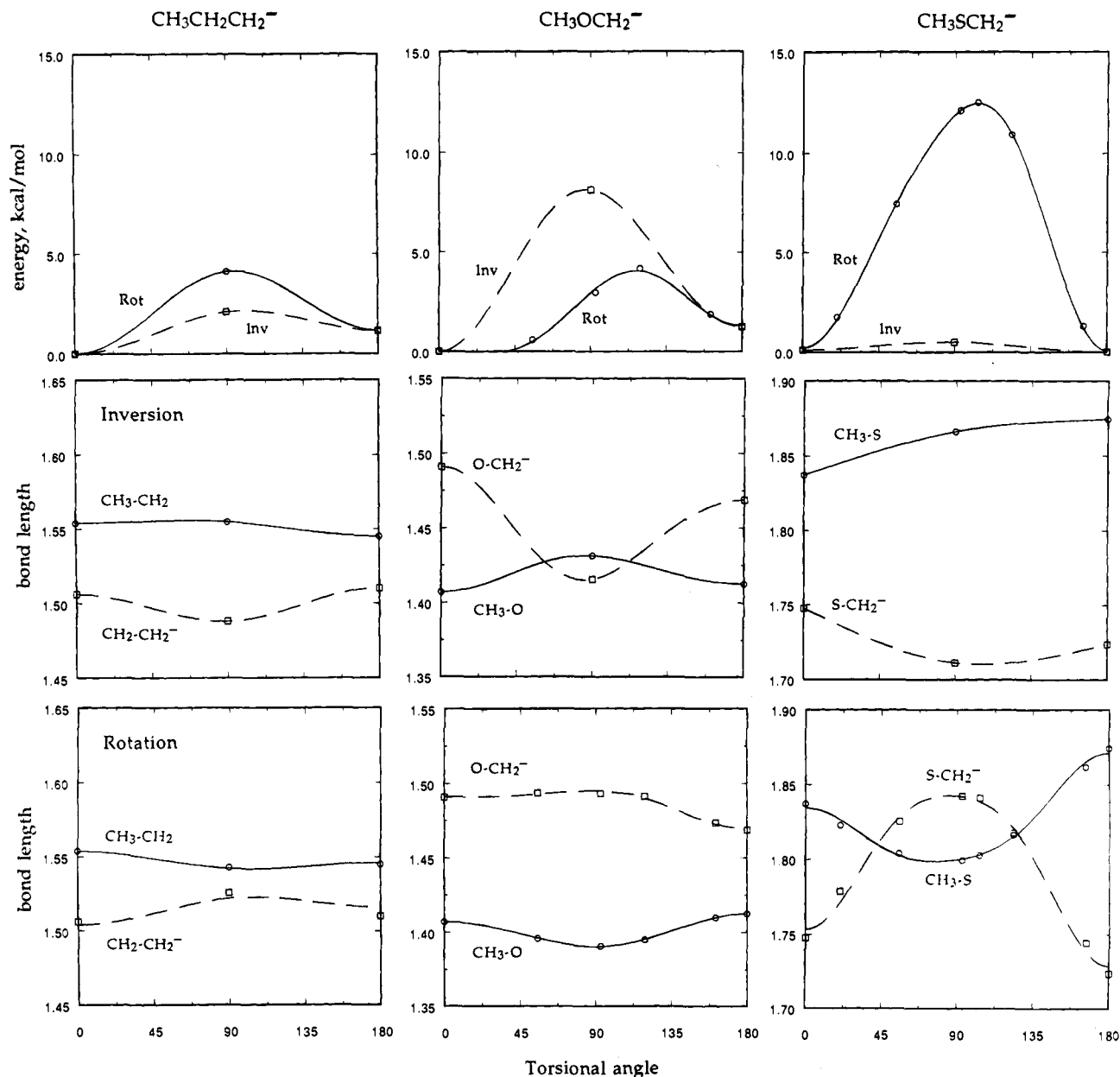


Figure 2. Rotation and inversion barriers for the anions of propane, dimethyl ether, and dimethyl sulfide.

parameters. The conversion of the parent molecules to the corresponding radicals leads to a common set of structural changes (Figure 1). The radical center orients itself so as to minimize its interaction with the lone pairs on oxygen or sulfur. The bond to the CH_3 group is relatively unchanged, whereas the bond to the radical center is shortened. This may be due to the change in hybridization at that center, with the radical placed in a largely p orbital and the $\text{C}-\text{O}$ or $\text{C}-\text{S}$ bond being made using an approximately sp^2 orbital. Increased s character leads to shorter bonds.¹⁴ Essentially all of the spin density in the radicals was calculated to be at the carbon. It might be noted that the change in bond length on going from the parent to the radical is significantly larger for dimethyl sulfide (0.092 Å) than for dimethyl ether (0.055 Å) whereas for a hybridization change at carbon one might expect the two to be approximately equal.

The anions do not present such a simple picture. The anion from dimethyl ether (**1a**) has a plane of symmetry and a markedly pyramidal methylene carbon (away from the methyl

group with a pyramidalization angle, α , of 64.6°) resembling that of typical unstabilized carbanions (the propyl anion at the same level of theory has $\alpha = 45.6^\circ$). The $\text{O}-\text{CH}_2^-$ bond length is relatively long (1.490 Å), whereas the other $\text{C}-\text{O}$ bond length is close to that of 1. Both the conformation and the bond length suggest a repulsive interaction between the lone pair at carbon and the lone pairs at oxygen. This might also be expressed as a repulsion between the negative charge at carbon and the partial negative charge at oxygen that results from its electronegativity. The barrier for rotation about the $\text{O}-\text{CH}_2^-$ bond is shown in Figure 2 and was found to be 4.2 kcal/mol. The changes in bond lengths on rotation also are shown in Figure 2 and are relatively small. The pyramidalization angle changes only slightly on rotation ($\alpha = 63.7^\circ$ at $\tau = 93^\circ$ and $\alpha = 60.9^\circ$ at $\tau = 180^\circ$).

It is also possible to change the conformation at the methylene group by inversion, and here the barrier was found to be 10.2 kcal/mol. Thus, rotation is preferred over inversion. It is interesting to compare these barriers with those for the 1-propyl anion: rotation = 4.3 kcal/mol and inversion = 2.1 kcal/mol.¹⁵

(13) Curtiss, L. A.; Raghavachari, K.; Pople, J. A. *J. Chem. Phys.* **1993**, *98*, 1293.

(14) Coulson, C. A. *Valence*, Oxford University Press: Oxford, 1952.

The rotational barrier is essentially the same as for the ether anion. However, the large inversion barrier for the ether anion shows that there is some interaction between O and CH_2^- which requires the methylene group to be pyramidal. Since pyramidalization of the methylene group is not affected by rotation about the C–O bond, it must result from a σ interaction. Oxygen is more electronegative than carbon, and therefore it would be expected to prefer to be bonded to a carbon orbital with high p character.¹⁶ This allows the carbon to place the lone pair in an orbital with relatively high s character and leads to a large pyramidalization angle. Inversion of configuration will then lead to an sp^2 hybridized carbon at the transition state, and the increase in s character will lead to an increase in energy as compared to the 1-propyl anion, as well as a decrease in the O– CH_2^- bond length.

The anion from dimethyl sulfide (**2a**) is much closer to being planar ($\alpha = 31.3^\circ$) and is pyramidalized toward the methyl group. Here, the difference in energy between $\tau = 0^\circ$ and 180° is small. Further, the pattern of C–X bond lengths found with **1a** is reversed in **2a**. The C–S bond to the methyl group is long (1.874 Å) and the bond to the methylene group is short (1.722 Å). Similar changes were found in going from dimethyl sulfoxide (**3**) and dimethyl sulfone (**4**) to their anions. Both **2** and **4** give a relatively large increase in S– CH_3 bond length on going to the anion, but the change with **3** was quite small. The data show that whereas there is a repulsive interaction with the anionic center in **1a**, there is an attractive interaction in **2a**, **3a**, and **4a**. It may also be noted that the pyramidalization is smaller for all of these anions than for **1a** or the 1-propyl anion.

The barrier to rotation about the S– CH_2^- bond of the anion from dimethyl sulfide is shown in Figure 2.¹⁷ Here, the rotational barrier was found to be 12.5 kcal/mol, much larger than for the anion from dimethyl ether. At the same time, there are large changes in bond lengths (Figure 2) so that the order of the CH_3 –S and S– CH_2^- lengths inverts during the course of rotation. The pyramidalization angle also changes markedly on rotation going from $\alpha = 31.3^\circ$ at $\tau = 0^\circ$ to $\alpha = 61.5^\circ$ at $\tau = 93^\circ$ and $\alpha = 36.5^\circ$ at $\tau = 180^\circ$. On the other hand, inversion was found to have a barrier of only 0.5 kcal/mol. In this case, inversion is the low-energy process that leads to conformational change. The small inversion barrier coupled with the large rotational barrier and the bond length changes indicates a strong interaction between the CH_3 –S bond and CH_2^- that requires the lone pair to be close to the C–S–C plane. The difference between S and O in their interaction with a CH_2^- group is striking.

It seemed possible that something could be learned by examining the dependence of the rotation and inversion barriers on the basis set used in the calculations. Here, it would be necessary to use only HF calculations since the inclusion of electron correlation can, in effect, simulate the addition of functions with higher angular momentum.¹⁸ The results of a set of calculations are summarized in Table 2. It can be seen that a significant barrier is found even at the 6-31G level. Diffuse functions (+) raise the rotational barrier a little, and d polarization functions (*) raise it considerably more. Diffuse

Table 2. Calculated Rotation and Inversion Barriers for $\text{CH}_3\text{SCH}_2^-$ (kcal/mol)

basis set	rotation barrier	inversion barrier
6-31G	6.7	5.2
6-31+G	7.8	3.2
6-31G*	10.8	4.7
6-31+G*	9.8	2.2
MP2/6-31+G	11.4	
MP2/6-31+G*	12.5	0.5

functions lower the inversion barrier and d functions reduce it further. The effects of diffuse and d functions are not additive.

3. Charge Distribution and Bond Orders

An analysis of the molecular orbitals presents problems in that it is difficult to sort out the many changes that occur on going to the anions. These problems further increase when correlated wave functions are used. Therefore, we prefer to carry out analyses of charge density distributions that may be derived from MO calculations. They are experimental quantities that may also be obtained from X-ray diffraction studies,¹⁹ and thus are especially well suited to an analysis of the changes that occur.²⁰ Two methods have been used. The first is Bader's theory of atoms in molecules²¹ in which the electron populations at atoms are obtained by integration of the charge density over properly defined atomic volumes.

The atomic charges derived from the electron populations are summarized in Table 3. As expected, the electronegative oxygen in **1** leads to relatively large positive charges at the carbons. The formation of the anion, **1a**, does not lead to much change at oxygen, and most of the charge remains at the methylene carbon. This is best seen in the second part of Table 3 that gives the charge shifts for each of the groups. The large charge at carbon is in accord with the pyramidal nature of the methylene group which is similar to that of the propyl anion. The lack of change at oxygen probably results from it being essentially "saturated" with charge, and therefore unable to accept any more.

The change in charges for dimethyl sulfide is quite different than those for dimethyl ether. The methyl groups in **2** have total charges of -0.013 e and the sulfur has a charge of $+0.028$. The small difference in charge corresponds to the small difference in electronegativity between carbon and sulfur. It can be seen from Table 3 that the net change for going from **2** to its anion is small at sulfur (0.1 e) and large for the anionic center. There is also considerably more charge transfer to the methyl group in **2a** than in **1a**.

The charge at the CH_2^- group decreases in the order **1a** > **2a** > **3a** > **4a**, corresponding to the increases in acidity. The sulfur and oxygen help bear the negative charge in both **3a** and **4a**. As a further check on the conclusions derived from the electron populations, the atomic charges also were obtained using the natural population analysis of Weinhold and Reed.²² The change in charge on going from the parent to the anions is given in Table 3, and the values are in good agreement with those derived by integrating the charge density.

(15) The MP2(fc)/6-31+G* energies for the rotation and inversion transition states for 1-propyl anions were -117.98106 and -117.98450 hartrees, respectively.

(16) Bent, H. A. *Chem. Rev.* **1961**, *61*, 275.

(17) The barriers to rotation were examined for HSCH_2^- and HOCH_2^- in ref 9, but only at a lower theoretical level. Our results for the methylated derivatives are qualitatively similar, but quantitatively significantly different.

(18) For example, the charge distribution based on 1s AO's for the internuclear region of H_2 may be improved by the addition of p polarization functions, or by configuration interaction using the doubly excited configuration.

(19) Coppens, P. In *Electron Distributions in the Chemical Bond*; Hall, M. B., Ed.; Plenum Press: New York, 1982; pp 61–92.

(20) Wiberg, K. B.; Hadad, C. M.; Breneman, C. M.; Laidig, K. E.; Murcko, M. A.; LePage, T. J. *Science* **1991**, *252*, 1265.

(21) Bader, R. F. W. *Atoms in Molecules. A Quantum Theory*; Clarendon Press: Oxford, 1990. Biegler-König, F. W.; Bader, R. F. W.; Tang, T.-H. *J. Comput. Chem.* **1982**, *3*, 317.

(22) Reed, A. E.; Weinstock, R. B.; Weinhold, F. A. *J. Chem. Phys.* **1985**, *83*, 735. Reed, A. E.; Weinhold, F. *J. Chem. Phys.* **1986**, *84*, 2428. Reed, A. E.; Weinhold, F.; Curtiss, L. A. *Chem. Rev.* **1988**, *88*, 899.

Table 3. Calculated Charges and Charge Shifts

		Calculated Charges									
atom ^a	neutral	radical	anion			atom ^a	neutral	radical	anion		
			gs	inv. TS	rot. TS				gs	inv. TS	rot. TS
a. Dimethyl Ether (1)											
O	-1.104	-1.125	-1.113	-1.104	-1.101	C ₂	0.442	0.416	0.495	0.400	0.507
C ₁	0.442	0.401	-0.172	-0.223	-0.180	H _a	0.058	0.066	-0.037	-0.037	-0.018
H _a	0.058					H _b	0.026	0.041, 0.063	-0.011	-0.017	-0.014, -0.034
H _b	0.026	0.088, 0.050	-0.077	-0.002	-0.080, -0.080	sum	0.000	-0.002	-1.003	-1.002	-1.000
b. Dimethyl Sulfide (2)											
S	0.028	0.171	-0.068	-0.053	-0.150	C ₂	-0.183	-0.182	-0.231	-0.226	-0.193
C ₁	-0.183	-0.378	-0.629	-0.689	-0.601	H _a	0.066	0.070	-0.016	-0.021	+0.057
H _a	0.066					H _b	0.052	0.062, 0.068	-0.002	+0.001	+0.009, +0.029
H _b	0.052	0.090, 0.097	-0.026	-0.006	-0.049, -0.050	sum	0.002	-0.001	-1.000	-0.999	-0.999
c. Dimethyl Sulfoxide (3)											
S	1.296	1.359	1.086			C ₂	-0.240	-0.229	-0.216		
O	-1.282	-1.277	-1.339			H _a	0.082	0.094	0.038		
C ₁	-0.240	-0.353	-0.620			H _b	0.066	0.071	0.032		
H _a	0.082	0.138	0.007			H _c	0.086	0.086	0.026		
H _b	0.066	0.108	-0.002			sum	0.003	-0.002	-0.987		
H _c	0.086										
d. Dimethyl Sulfone (4)											
S	2.547	2.596	2.406			C ₂	-0.230	-0.226	-0.221		
O	-1.336	-1.332	-1.392			H _a	0.113	0.113	0.041		
C ₁	-0.230	-0.295	-0.560			H _b	0.090	0.093	0.030		
H _a	0.113					sum	0.001	-0.002	-1.000		
H _b	0.090	0.143	0.029								
e. Propane											
C ₁	-0.075	-0.179	-0.575	-0.650	-0.628	C ₃	-0.075	-0.074	-0.124	-0.122	-0.092
H _a	0.023					H _a	0.023	0.025	-0.060	-0.070	-0.042
H _b	0.020	0.058	-0.072	-0.032	-0.075, -0.068	H _b	0.020	0.025	-0.020	-0.018	0.000, -0.013
C ₂	0.002	0.010	0.019	0.032	0.014	sum	0.002	-0.002	-1.002	-1.000	-1.003
H	0.012	0.025	-0.039	-0.045	-0.054, -0.045						
Charge Shifts											
group	neutral → radical	radical → anion	neutral → anion ^b	group	neutral → radical	radical → anion	neutral → anion ^b				
a. Dimethyl Ether											
O	-0.021	+0.012	-0.009 (-0.087)	CH ₃	+0.034	-0.150	-0.116 (-0.085)				
CH ₂	-0.013	-0.865	-0.878 (-0.827)								
b. Dimethyl Sulfide											
S	+0.143	-0.239	-0.096 (-0.100)	CH ₃	-0.031	-0.269	-0.238 (-0.180)				
CH ₂ ⁻	-0.177	-0.491	-0.668 (-0.720)								
c. Dimethyl Sulfoxide											
S	+0.063	-0.273	-0.209	CH ₂ ⁻	-0.101	-0.508	-0.608				
O	+0.005	-0.062	-0.057	CH ₃	+0.028	-0.142	-0.113				
d. Dimethyl Sulfone											
S	+0.049	-0.190	-0.141	CH ₂ ⁻	-0.072	-0.493	-0.563				
O	+0.004	-0.060	-0.055	CH ₃	+0.010	-0.193	-0.183				
e. Propane											
CH ₃	0.014	-0.222	-0.212	CH ₂ ⁻	-0.027	-0.656	-0.707				
CH ₂	0.033	-0.117	-0.084								

^a H_a is the in-plane hydrogen and H_b are the out-of-plane hydrogens. H_a at C₁ is lost on going to the radical or anion. ^b Values in parentheses were derived from the natural population analysis.

The covalent bond orders²³ are perhaps the most interesting quantities (Table 4). On going from **1** to **1r** or **1a**, there are essentially no changes in the C–O bond orders. However, with **2**, **3**, or **4**, the formation of the anion leads to a large increase in the bond order for the S–CH₂⁻ bond without much change in the CH₃–S bond. This clearly indicates that the anionic center interacts with the sulfur to give additional bonding character.

The bond length changes are also reflected in the calculated stretching force constants. In dimethyl ether, the C–O stretching constant is 6.67 mdyne/Å, and in the anion, the H₃C–O constant is relatively unchanged at 7.08, whereas the O–CH₂⁻ constant has decreased to 3.97 mdyne/Å, corresponding to the considerable increase in bond length. In dimethyl sulfide, the C–S stretching constant is 3.80 mdyne/Å, and in its anion the

H₃C–S constant is 3.00 and the S–CH₂⁻ constant is 3.46 mdyne/Å. Here the latter is the larger constant corresponding to the smaller C–S bond length.

The second, and independent, way of examining the changes that occur on going from **1** or **2** to their anions makes use of charge density difference plots. Here, the main problem is that the two species being compared must have their atoms at the same positions so that the small changes that occur on bonding are to be seen. One way is to compare the radical and the anion, both calculated at the anion geometry. This would correspond to the vertical ionization of an electron from the anion. The radicals calculated at the anion geometries have significantly

(23) Cioslowski, J.; Mixon, S. T. *J. Am. Chem. Soc.* **1991**, *113*, 4142. Wiberg, K. B.; Hadad, C. M.; Rablen, P. R.; Cioslowski, J. *J. Am. Chem. Soc.* **1992**, *114*, 8644.

Table 4. Covalent Bond Orders^a

compd	bond	neutral	radical	anion
dimethyl ether	C ₁ -O	0.860	0.897	0.882
	C ₂ -O	0.860	0.834	0.894
dimethyl sulfide	C ₁ -S	1.099	1.228	1.396
	C ₂ -S	1.099	1.078	1.083
dimethyl sulfoxide	C ₁ -S	1.010	1.075	1.368
	C ₂ -S	1.010	0.987	0.991
	S-O	1.265	1.263	1.212
dimethyl sulfone	C ₁ -S	0.962	0.982	1.315
	C ₂ -S	0.962	0.963	0.910
	S-O	1.119	1.119	1.063
propane	C ₁ -C ₂	1.002	1.043	1.108
	C ₂ -C ₃	1.002	0.981	0.981

^a The hydrogen is taken from C₁ in each case.

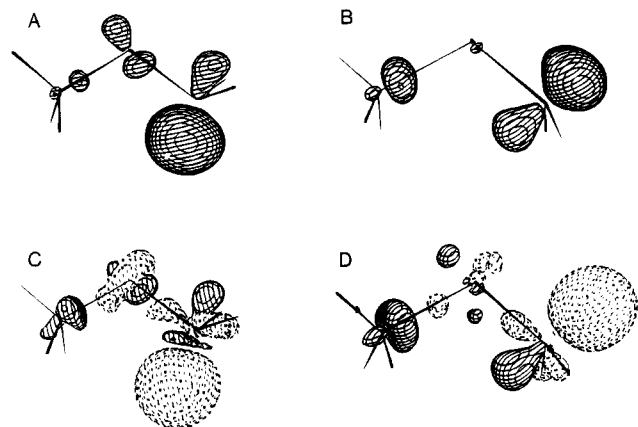


Figure 3. Charge density difference plots for the anions-radicals derived from dimethyl ether (A) and dimethyl sulfide (B) and for the corresponding anions-precursors (C and D). The contour level is $1 \times 10^{-2} e/\text{au}^3$ and in each case the structures were based on the optimized geometries for the anions.

increased energies, but this is largely due to the difference in bond lengths. The latter should not have a major effect on the charge distributions.

It was seen in Table 3 that the changes in charge on going from 1 to the radical are fairly small and that the large change is seen on going from the radical to the anion. The changes in charge are made more clear by plotting the difference in charge density on going from the radical to the anion, and this is shown in Figure 3. The electron that was added to the radical appeared largely at the carbon. The conformation at the anionic site is that which will minimize repulsion between the lone pairs at oxygen and the lone pair at the anionic carbon.

The shift in charge on forming the anion may also be examined by comparing the anions with their parent molecules. These changes also are shown in Figure 3. The large depletion zone (dashed contours) in the vicinity of the lone pair corresponds to the contraction of charge on going from the C-H bond to the C-lone pair. The rest of the contours are similar to those of the anion-radical, and again show a shift of charge density toward the terminal methyl group in 2a.

There remains the question whether or not there might be a significant charge shift resulting from the use of the anion geometry for the calculations on the radicals and the neutral precursors. This was examined by keeping just the terminal methyl groups constant and allowing the rest of each molecule to adopt its preferred geometry. Charge density difference plots for the vicinity of the methyl groups are shown in Figure 4. Here again, the sulfide still gives a considerable charge shift to the terminal methyl group, but the ether gives only a very small charge shift.

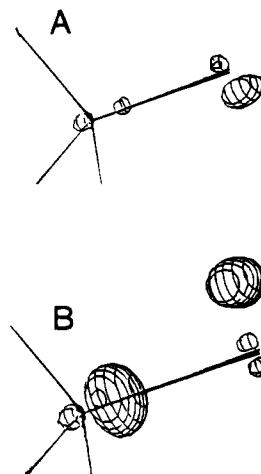


Figure 4. Charge density difference plots for the terminal methyl groups of the anions-precursors for dimethyl ether (A) and dimethyl sulfide (B). The only structural constraint was on the terminal methyl groups. The contour level is $1 \times 10^{-2} e/\text{au}^3$.

Table 5. Calculated Energies of Lithium Salts

compd	HF/6-31G*	MP2/6-31+G*	ZPE ^a
CH ₃ OCH ₂ Li	-160.898 65	-161.362 85	41.0
CH ₃ SCH ₂ Li	-483.570 58	-483.975 78	38.6
(CH ₃) ₂ O-Li ⁺	-161.366 21	-161.813 57	49.6
(CH ₃) ₂ S-Li ⁺	-484.020 30	-484.409 31	46.7

^a Based on HF/6-31G* frequencies scaled by 0.893.

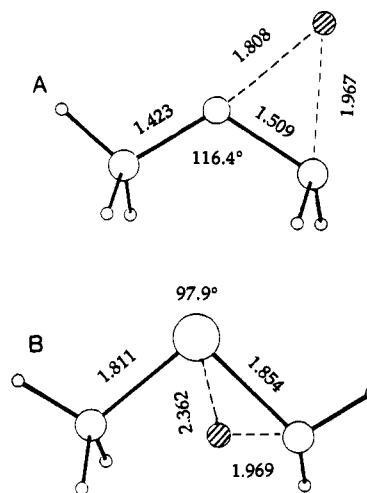


Figure 5. Structures of lithio derivatives obtained from 1 (A) and 2 (B). The lithiums are shaded.

4. Lithium Salts

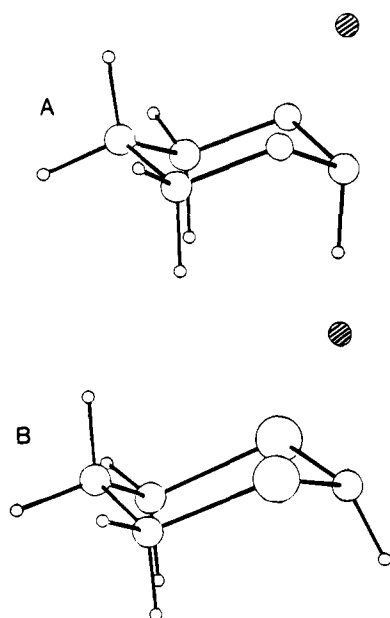
Schleyer et al.²⁴ have shown that it is frequently useful to compare carbanions with the corresponding lithium salts. Therefore we have obtained the MP2/6-31+G* geometries and energies for methoxymethyl lithium (5) and thiomethoxymethyl lithium (6) (Table 5). The structures are shown in Figure 5. It is interesting to note the difference in the preferred location of the lithium cation in the two cases. A comparison with Figure 1 shows a dramatic shift in the C-S bond length on going from the anion, 2a, to the lithium salt, 6. The S-CH₂⁻ bond is relatively short in 2a, whereas the S-CH₂Li bond is relatively long in 6. At the same time, the S-C bond order decreases from 1.396 to 1.152. It is clear that the nature of the S-CH₂⁻

(24) Schleyer, P. v. R.; Chandrasekhar, J.; Kos, A. J.; Clark, T.; Spitznagel, G. W. *J. Chem. Soc., Chem. Commun.* **1981**, 882. The lithium salts LiCH₂SH and LiCH₂OH were studied in ref 7 at the HF/3-21+G level.

Table 6. Calculated Energies of 1,3-Dioxane, 1,3-Dithiane, and Their Carbanions

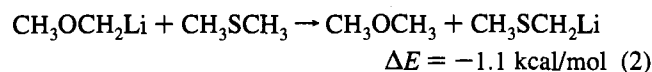
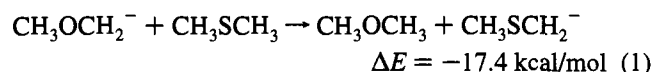
compd	ZPE ^a	MP2/6-31G*	MP2/6-311++G**	ΔH_{acid}^c
1,3-dioxane	74.6	-306.702 75	-308.905 49 ^b	408
anion	64.1	-306.014 56	-306.238 29	
lithium salt	66.8	-313.552 96	-313.748 22	
1,3-dithiane	69.8	-951.918 12	-952.106 16	380
anion	60.8	-951.281 88	-951.485 56	
lithium salt	63.1	-958.791 86	-958.979 61	

^a Based on HF/6-31G* frequencies scaled by 0.893. ^b The MP2/6-311++G** energies were obtained at the MP2/6-31G* geometries. ^c The ΔH_{acid} values were obtained from the MP2/6-311++G** energies plus a correction for the change in zero-point energies.

**Figure 6.** Structures of lithio derivatives derived from 1,3-dioxane (A) and 1,3-dithiane (B). The lithiums are shaded.

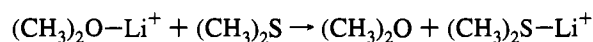
bond has been changed by the localization of charge that occurs in the lithium salt.

The effect of the lithium cation also may be seen in the following exchange reactions:



The considerable stabilization of **2a** vs. **1a** that is seen in the gas phase appears to be lost on going to the lithium salts. This may be due either to a decreased interaction between S and CH_2^- in the lithium salt, as suggested by the change in bond order, or to a greater chelation of lithium by the oxygen in **1a** as compared to the sulfur in **2a**.

One way in which to test the chelation hypothesis is to examine the reaction

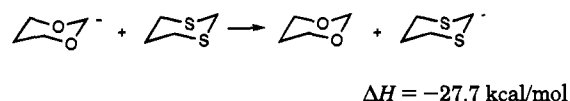


Geometry optimizations at the HF/6-31G* level found the lithium to lie in the C–O–C plane and on the bisector of the C–O–C angle for the ether. With the sulfide, the lithium was in the plane that bisected the C–S–C angle, but it was 54.3° from the bisector. The energy change at the MP2/6-31+G* level was +9.7 kcal/mol, about half of the difference between reactions 1 and 2 above. Thus, the effect of the lithium cation

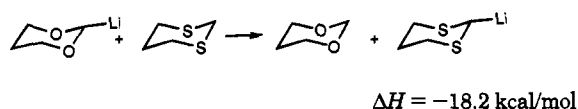
on reactions 1 and 2 may well involve more than just the chelation energy, as is suggested by the change in bond order.

The energy change for reaction 2 suggests that there should be little difference in the equilibrium constants for the removal of a proton from **1** or **2** with the formation of the lithium salt in a non-complexing solvent. The formation of an anion next to sulfur is usually carried out using a compound such as 1,3-dithiane. In common practice, dithiane is converted to its lithium salt by reaction with butyllithium in tetrahydrofuran.² In order to have an estimate of the difference in acidity between 1,3-dioxane (**5**) and 1,3-dithiane (**6**), geometry optimizations were carried out at the MP2/6-31G* level giving the results presented in Table 6. The zero-point energies were obtained from 6-31G* frequency calculations. The structures of the compounds are shown in Figure 6. MP2/6-311++G** energies were obtained using the calculated structures.

The proton transfer energy for these compounds is whereas



the corresponding lithium cation transfer energy is Here, the



1,3-dithiane is considerably more acidic than 1,3-dioxane both in the gas phase and when the anions are in the form of lithium salts.

5. Discussion

The structural data, the bond orders, and the rotational barriers clearly indicate a difference between O and S in the way in which they interact with a CH_2^- group. In the anion formed from dimethyl ether, the O– CH_2^- bond is long and the CH_3 –O bond is slightly reduced in length. However, in the anion formed from dimethyl sulfide, the S– CH_2^- bond is short and the CH_3 –S bond is relatively long. The O– CH_2^- bond order does not significantly change on going from dimethyl ether to its anion, whereas the S– CH_2^- bond order increases from 1.1 to 1.4 on going from dimethyl sulfide to its anion. These changes in the S– CH_2^- bond essentially disappear on forming the lithium salt in which the negative charge is more localized.

These data strongly suggest that the CH_2^- group donates charge to the CH_3 –S bond, but the question of which sulfur orbitals are involved is not clear. Both Lehn and Wipff⁵ and Schleyer et al.⁷ found that although the inclusion of d orbitals at sulfur in the basis set led to significant changes in structure, it did not lead to significant changes in relative energies. Some additional data are shown in Table 7. The energy comparisons agree with these observations. Although the inclusion of diffuse s and p functions (+) improves the calculated relative energies of the parents and their anions, these functions have a relatively small effect on the total energy. On the other hand, the change in energy on going from dimethyl sulfide to its anion is not significantly affected by the inclusion of d functions (*) in the basis set. Nevertheless, the inclusion of these functions leads to dramatic changes in geometry both for the sulfide and its anion, and also leads to significant changes in the bond orders for the S– CH_2^- bond. The large decrease in the MP2 energies when d functions are included (132 kcal/mol) for both the sulfide and the anion indicate that these functions play an important role. However, they are not more important for the anion than

Table 7. Effect of Basis Set on Calculated Properties of Dimethyl Sulfide and Its Anion

basis set	anion		parent	anion		parent
	CH ₃ -S	S-CH ₂ ⁻	CH ₃ -S	CH ₃ -O	OCH ₂ ⁻	CH ₃ O
a. Bond Lengths						
HF/6-31G	1.895	1.918	1.869	1.398	1.552	1.423
HF/6-31+G	1.901	1.765	1.868	1.407	1.506	1.426
HF/6-31G*	1.841	1.776	1.808	1.362	1.519	1.392
HF/6-31+G*	1.842	1.765	1.808	1.371	1.478	1.393
MP2/6-31+G	2.210	1.795	1.893	1.460	1.551	1.473
MP2/6-31+G*	1.874	1.722	1.807	1.407	1.490	1.420
b. Bond Orders						
basis set	anion		parent	anion		parent
	CH ₃ -S	S-CH ₂ ⁻	CH ₃ -S	CH ₃ -O	OCH ₂ ⁻	CH ₃ O
HF/6-31G	1.093	1.061	1.087			
HF/6-31+G	1.086	1.137	1.087			
HF/6-31G*	1.126	1.264	1.126			
HF/6-31+G*	1.125	1.299	1.127			
MP2/6-31+G	1.029	1.352	1.061			
MP2/6-31+G*	1.083	1.368	1.099	0.894	0.882	0.860
basis set	dimethyl sulfide			dimethyl ether		
	anion	parent	ΔE^a	anion	parent	ΔE^a
HF/6-31G	-475.990 65	476.668 52	425.4	-153.288 90	-153.994 70	442.9
HF/6-31+G	-476.010 34	-476.670 05	414.0	-153.318 70	-153.999 30	427.1
HF/6-31G*	-476.058 25	-476.735 33	424.9	-153.353 49	-154.064 75	446.3
HF/6-31+G*	-476.078 28	-476.736 61	413.0	-153.382 79	-154.069 43	430.9
MP2/6-31+G	-476.270 21	-476.915 49	404.9	-153.646 25	-154.312 74	418.2
MP2/6-31+G*	-476.483 16	-477.125 89	403.3	-154.844 08	-154.514 63	420.8

^a Not corrected for zero-point energy changes.

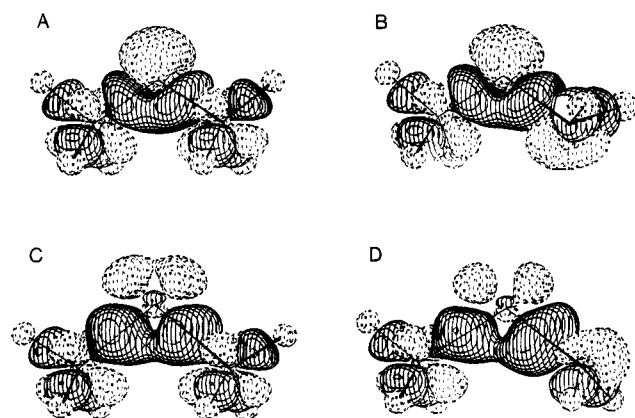


Figure 7. Charge density difference maps for MP2/6-31+G* - MP2/6-31+G showing the effect of d functions (*) on the charge density distribution for dimethyl ether (A), dimethyl sulfide (C), and their anions (B and D). The contour level is 4×10^{-3} e/au³.

for dimethyl sulfide itself, and as a result they do not contribute significantly to the increased acidity of dimethyl sulfide.

The emphasis on orbitals is probably the major reason for the difficulty chemists have had in explaining the difference between sulfur and oxygen. Properly, the only role the basis functions (incorrectly called atomic orbitals) play in the calculations is to allow the electron density distribution to be described as accurately as possible. The properties of a molecule at its equilibrium geometry depend only on this distribution. So, rather than asking which "orbitals" are used, it would seem more appropriate to ask how the electron density distribution changes as the flexibility of the basis set is increased. This may be examined with the use of charge density difference maps.

Figure 7 shows density difference plots between MP2/6-31+G* and MP2/6-31+G wave functions for 1, 2, and their anions and reveals the effect of including d basis functions. It can be seen that the change in charge density distribution is

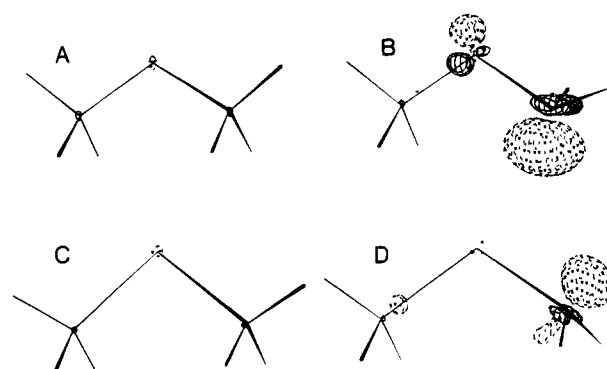


Figure 8. Charge density difference maps for MP2/6-31+G* - MP2/6-31G* showing the effect of diffuse functions (+) on the charge density distribution for dimethyl ether (A), dimethyl sulfide (C), and their anions (B and D). The contour level is 1×10^{-2} e/au³.

similar for a compound and its anion, and thus leads to similar but large changes in energy. The correspondence between 1 and 2 is interesting. In the ether 1, the inclusion of d functions leads to a shift of charge density from the oxygen lone pair into the O-C bonds. In 2, there is a similar increase in charge density in the C-S bonds, and again the charge density is taken from a region that might best be described as sulfur lone pairs. It can be seen that the d functions do act as polarization functions that allow charge density to be shifted into regions that improve bonding. These conclusions are in good agreement with a recent theoretical study of the role of d functions.²⁵

The effect of diffuse functions (+) is shown in Figure 8 via charge density difference plots between MP2/6-31+G* and MP2/6-31G* wave functions. Here, the effects are minimal for 1 and 2 and are localized in the region of the anionic sites for 1a and 2a.

6. Conclusions

The enhanced acidity of dimethyl ether as compared to propane is due to the electronegativity of oxygen. The latter also leads to increased pyramidalization of the methylene group and a significantly larger inversion barrier for the methoxy-methyl anion **1a**. The rotational barrier is about as large as for the 1-propyl anion, and no significant change in pyramidalization occurs during rotation about the O-CH₂⁻ bond. There is no indication of an important π interaction.

In contrast to dimethyl ether, the anion (**2a**) derived from dimethyl sulfide has a small degree of pyramidalization at the methylene group and has a negligible inversion barrier. Here, the S-CH₂⁻ rotational barrier is considerably increased. During rotation, the S-CH₂⁻ bond length is markedly changed, and the pyramidalization angle increases substantially. Clearly, the main interaction is π in character, and it is best described as hyperconjugation. In accord with this, the S-CH₂⁻ bond order is 1.4, indicating significant double bond character.

The observation of negative hyperconjugation with CH₃SCH₂⁻ and not CH₃OCH₂⁻ can be related to the difference between the CH₃-O and CH₃-S σ^* orbitals. According to the natural bond orbital analysis,²² the energy of the anionic lone pair in **1a** (-0.1061 H) is only slightly lower than that of the lone pair in **2a** (-0.0388 H). However, the CH₃-O σ^* orbital in **1a** has a much higher energy (+0.8014 H) than the CH₃-S σ^* orbital in **2a** (+0.5296 H). Thus the difference in energy between the lone pair and the σ^* orbital in **2a** is considerably smaller than that for **1a**, allowing a stronger interaction.

It is interesting to note that the AIM analysis for the 1-propyl anion suggests some charge transfer to the terminal methyl group, and this is also found in charge density difference maps. In the rotational transition state the charge at the terminal methyl

group is decreased from -0.224 in the ground state to -0.148, indicating some participation of negative hyperconjugation. Here, the energy of the anionic lone pair is -0.0222 H and that of the CH₃-CH₂ σ^* orbital is +0.8250 H. The difference is smaller than for **1a**, allowing more charge transfer. Another factor is the nature of the σ^* orbital. In the 1-propyl anion and **2a** the σ^* orbital would be expected to have about equal coefficients at the two atoms because of the similar electronegativity. However, with **1a**, the CH₃-O σ orbital will have the larger coefficient at O, and accordingly, the CH₃-O σ^* orbital will have the larger coefficient at carbon. With this carbon removed from the anionic center, the coupling matrix element should be smaller than for the other anions, leading to a weaker interaction.

Experimental Section

Calculations. The ab initio calculations were carried out using GAUSSIAN-92.²⁶ The AIM charge density integrations were carried out using PROAIM,²¹ and the NPA charges and the Natural Bond Orbital Analysis were obtained via the Weinhold-Reed code²² contained in GAUSSIAN-92. The bond orders were obtained using the program BONDER.²³ Charge density difference plots were made using locally developed programs.²⁷

Acknowledgment. This investigation was supported by the National Institutes of Health.

(26) Frisch, M. J.; Trucks, G. W.; Head-Gordon, M.; Gill, P. M. W.; Wong, M. W.; Foresman, J. B.; Johnson, B. G.; Schlegel, H. B.; Robb, M. A.; Replogle, E. S.; Gomperts, R.; Andres, J. L.; Raghavachari, K.; Binkley, J. S.; Gonzalez, C.; Martin, R. L.; Fox, D. J.; Defrees, D. J.; Baker, J.; Stewart, J. J. P.; Pople, J. A. GAUSSIAN 92, Revision A, Gaussian, Inc.: Pittsburgh, PA, 1992.

(27) Hadad, C. M. and Rablen, P. R., Yale University.